Myo/Nog Cells Give Rise to Myofibroblasts During Epiretinal Membrane Formation in a Mouse Model of Proliferative Vitreoretinopathy

Mara Crispin,[1] Jacquelyn Gerhart,[1] Alison Heffer,[2] Mark Martin,[1] Fathma Abdalla,[1] Arturo Bravo-Nuevo,[1] Nancy J. Philp,[3] Ajay E. Kuriyan,[2,4] and Mindy George-Weinstein[1]

[1]Philadelphia College of Osteopathic Medicine, Philadelphia, Pennsylvania, United States
[2]Flaum Eye Institute, University of Rochester Medical Center, Rochester, New York, United States
[3]Sydney Kimmel Medical School of Thomas Jefferson University, Philadelphia, Pennsylvania, United States
[4]Current address: Retina Service/Mid Atlantic Retina, Wills Eye Hospital, Thomas Jefferson University, Philadelphia, Pennsylvania, United States

Correspondence: Mindy George-Weinstein, Philadelphia College of Osteopathic Medicine, 307 Rowland Hall, 4190 City Avenue, Philadelphia 19131, USA; mindygw@pcom.edu.

MC and JG contributed equally to the work.
AEK and MGW should be considered co-senior authors.

Received: August 31, 2022
Accepted: December 19, 2022
Published: February 1, 2023

Citation: Crispin M, Gerhart J, Heffer A, et al. Myo/Nog cells give rise to myofibroblasts during epiretinal membrane formation in a mouse model of proliferative vitreoretinopathy. *Invest Ophthalmol Vis Sci.* 2023;64(2):1. https://doi.org/10.1167/iovs.64.2.1

Purpose. Myo/Nog cells are the source of myofibroblasts in the lens and synthesize muscle proteins in human epiretinal membranes (ERMs). In the current study, we examined the response of Myo/Nog cells during ERM formation in a mouse model of proliferative vitreoretinopathy (PVR).

Methods. PVR was induced by intravitreal injections of gas and ARPE-19 cells. PVR grade was scored by fundus imaging, optical coherence tomography, and histology. Double label immunofluorescence localization was performed to quantify Myo/Nog cells, myofibroblasts, and leukocytes.

Results. Myo/Nog cells, identified by co-labeling with antibodies to brain-specific angiogenesis inhibitor 1 (BAI1) and Noggin, increased throughout the eye with induction of PVR and disease progression. They were present on the inner surface of the retina in grades 1/2 PVR and were the largest subpopulation of cells in grades 3 to 6 ERMs. All α-SMA-positive (+) cells and all but one striated myosin+ cell expressed BAI1 in grades 1 to 6 PVR. Folds and areas of retinal detachment were overlain by Myo/Nog cells containing muscle proteins. Low numbers of CD18, CD68, and CD45+ leukocytes were detected throughout the eye. Small subpopulations of BAI1+ cells expressed leukocyte markers. ARPE-19 cells were found in the vitreous but were rare in ERMs. Pigmented cells lacking Myo/Nog and muscle cell markers were present in ERMs and abundant within the retina by grade 5/6.

Conclusions. Myo/Nog cells differentiate into myofibroblasts that appear to contract and produce retinal folds and detachment. Targeting BAI1 for Myo/Nog cell depletion may be a pharmacological approach to preventing and treating PVR.

Keywords: Myo/Nog cells, proliferative vitreoretinopathy, myofibroblasts

Proliferative vitreoretinopathy (PVR) is characterized by the formation of membranes on the epiretinal or subretinal surface, and, in some cases, fibrotic tissue within the retina itself.[1–3] Contractions of these membranes produce a tractional force on the retina leading to detachment and possibly blindness.[1–4] PVR may arise in response to, or following repair of a rhegmatogenous retinal detachment.[1–3,5–7] Epiretinal membranes (ERMs) also may arise after a posterior vitreous detachment or proliferative diabetic retinopathy and uveitis. Whereas PVR membranes can be surgically removed, functional outcomes vary greatly, in part because of the potential for lasting structural and cellular damage.[1–3] To date, there are no pharmacological approaches for the prevention or treatment of PVR that have yielded consistent results.[1,3,8–10]

PVR membranes contain a variety of cell types, including glia, fibroblasts, leukocytes, fibroblast-like cells, and retinal pigment epithelial (RPE) cells.[1,2,6,10–17] Subpopulations of these cells are thought to transdifferentiate into contractile muscle-like cells called myofibroblasts.[4,5,13,16–22] Our analyses of human ERMs obtained from patients with a previous rhegmatogenous retinal detachment revealed that alpha smooth muscle actin (α-SMA), striated muscle myosin, and the skeletal muscle specific transcription factor myoblast determination factor 1 (MyoD) were exclusively expressed in a subpopulation called Myo/Nog cells.[23] The presence of differentiated Myo/Nog cells in human PVR membranes is consistent with the results of Shirpa et al.[24] who found a significant elevation of another member of the MyoD family, myogenic factor 6 (Myf6), in the vitreous of patients with rhegmatogenous retinal detachment compared to those with a macular hole and pucker.

Myo/Nog cells were first identified in the early embryo by their expression of the MyoD and the bone morphogenetic

protein (BMP) inhibitor Noggin.[25–27] A third marker of Myo/Nog cells is brain-specific angiogenesis inhibitor 1 (BAI1) recognized by the G8 monoclonal antibody (mAb).[25–29] Their expression of MyoD is the hallmark of Myo/Nog cell's commitment to the skeletal muscle lineage and capacity to differentiate into multinucleated skeletal muscle cells and single nucleated myofibroblasts.[30–33] Noggin released from Myo/Nog cells is critical for regulating the BMP signaling pathway.[25,34] Myo/Nog cells populate tissues throughout the embryo, including the eyes.[25,32,35] Depletion of Myo/Nog cells prior to the onset of gastrulation results in severe malformations of the body wall, central nervous system, and eyes.[25] Ocular defects include anophthalmia, microphthalmia, lens dysgenesis, and/or overgrowth of the retina.[25,35]

Adult tissues also contain Myo/Nog cells that become activated by stress and injury.[31,33,36–40] Cataract surgery induces the expansion and migration of the resident Myo/Nog population and their differentiation into myofibroblasts expressing multiple contractile proteins.[31,33] Contractions of myofibroblasts produce wrinkles in the lens capsule that impair vision in a condition called posterior capsule opacification (PCO).[41] Targeted depletion of Myo/Nog cells in the lens with the anti-BAI1 G8 mAb and complement, or G8 conjugated to 3DNA nanocarriers for the cytotoxin doxorubicin, prevents the emergence of myofibroblasts in cultures of human lens tissue and reduces PCO to clinically insignificant levels in rabbits.[31,33,42]

Myo/Nog cells also become activated in the retina in response to hypoxia and cell death.[38,39] In the mouse model of retinopathy of prematurity, targeted depletion of Myo/Nog cells increases photoreceptor cell death.[38] In a light damage model, injection of Myo/Nog cells into the rat vitreous promotes photoreceptor survival and function.[39] Similar neuroprotective activity of Myo/Nog cells was observed after focal injury to the rat brain.[40] Thus, the effects of Myo/Nog cells can be beneficial or pathologic depending on the environment and stimuli that trigger their activation.[25,31,33,35,38,39,43]

In this study, we examined the response of Myo/Nog cells in a mouse model of PVR induced by the combination of vitreous detachment caused by injection of gas and introduction of human ARPE-19 cells into the intravitreal space.[44] The grade of PVR in this model was classified by retinal thickening, formation of ERMs and retinal folds, and partial to complete retinal detachment.[44] ERMs that form following injection of gas and ARPE-19 cells resemble that of other species, including humans.[9,45] In this study, we tested the hypothesis that Myo/Nog cells are activated by the presence of ARPE-19 cells and are the source of myofibroblasts in ERMs and the retina.

Methods

PVR Induction

Eight- to 10-week-old, female C57BL/6J mice were purchased from Jackson Laboratory (Bar Harbor, ME, USA). All experiments adhered to the ARVO Statement for the Use of Animals in Ophthalmic and Vision Research and were approved by the University Committee of Animal Resources of the University of Rochester.

Intravitreal injections were performed as described previously[44] and diagrammed in Figure 1. Briefly, a puncture was made just posterior to the corneal-scleral junction using a 30 G needle. A 10 µL Hamilton syringe (Hamilton, Reno, NV, USA) and a 33 G needle were used to inject 0.5 µL of SF6 gas (Alcon Laboratories, Fort Worth, TX, USA) into the vitreous. One week later, the site where gas was injected was re-punctured and 1 µL of phosphate buffered saline (PBS) containing 2 to 8 $\times$ 10^4 human ARPE-19 cells[46] (ATCC, Manassas, VA, USA) or PBS alone was injected with a 10 µL Hamilton syringe and 33 G needle.

Analyses of PVR Development

PVR development and progression was characterized as described previously.[44] Fundus imagining was performed weekly. The pupil was dilated with an ophthalmic solution of phenylephrine 2.5% (Paragon Bioteck Inc., Portland, OR, USA) and tropicamide 1% (Akorn Inc., Lake Forest, IL, USA). GenTeal lubrication gel (Alcon, Fort Worth, TX, USA) was applied to prevent ocular surface drying. Eyes were imaged using the bright-field view of the Micron III Retinal Imaging System (Phoenix Instruments, Naperville, IL, USA) and StreamPix software (Norpix, Montreal, Quebec, Canada). The presence of vitreous and epiretinal cells and membranes, and changes in retinal structure were monitored by optical coherence tomography (OCT) after applying a contact lens using the Heidelberg Spectralis HRA + OCT imaging system (Heidelberg Engineering, Franklin, MA, USA).

Eyes were collected at 4 days or 1 to 4 weeks post injection of PBS or ARPE-19 cells, depending on PVR grade. Eyes

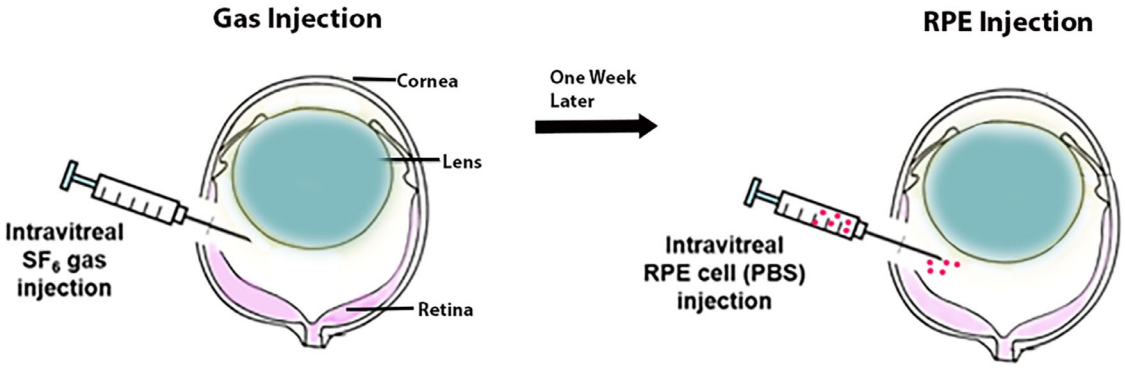

Figure 1. Procedure for inducing PVR. SF_6 gas was injected into the vitreous posterior to the corneal-scleral junction. Seven days later, the site where gas was injected was re-punctured and ARPE-19 cells introduced in PBS.

Investigative Ophthalmology & Visual Science

were fixed in 4% paraformaldehyde for 24 hours, washed, embedded in paraffin, and sectioned at 10 µM.

PVR Grading

PVR severity was based on previous grading schemes[47] and reproducible phenotypes observed in mice using fundus imagining, OCT, and histology.[44] All PBS injected control eyes had grade 0 PVR in which the retina appeared normal, cells were not observed in the vitreous, and membranes were not present. Grade 1 PVR was characterized by the presence of cells in the vitreous and on the inner retinal surface. In grade 2 PVR, cells had migrated to the blood vessels on the inner retinal surface and the retina was thickened. By grade 3 PVR, membranes had formed on the retinal surface and were accompanied by small pockets of subretinal fluid and/or focal areas of retinal elevation and folds. Grade 4 PVR exhibited multiple, focal retinal detachments involving less than 25% of the tissue and small pockets of subretinal fluid in close proximity to tractional ERMs on the surface of the retina. In grade 5 PVR, 25% to 75% of the retina was detached. Complete retinal detachment and a prominent, tractional ERM was present at grade 6 PVR.

Immunofluorescence Localization

Myo/Nog cells were identified in tissue sections by double labeling with the anti-BAI1 G8 IgM mouse mAb[30] and the anti-noggin goat polyclonal anti-serum (AF719; R&D Systems, Minneapolis, MN, USA), as described previously.[25,30] Double labeling also was carried out with the IgM BAI1 mAb and IgG mAb antibodies to α-SMA (F3777 diluted 1:250; Sigma-Aldrich, St. Louis, MO, USA), striated muscle myosin II (ab58899 diluted 1:200; Abcam, Cambridge, MA, USA), the leukocyte markers CD68 (ab201340 diluted 1:200; Abcam), CD45 (ab10558 diluted 1:200; Abcam), and CD18 (MA1819 diluted 1:100; ThermoFisher Scientific, Waltham, PA, USA), and human nucleoli (ab190710 diluted 1:100; Abcam). The α-SMA mAb was directly conjugated with fluorescein. Other primary antibodies were visualized with AffiniPure Fab fragment subclass and species-specific secondary antibodies conjugated with Rhodamine Red or Alexa 488 (Jackson ImmunoResearch Laboratories, Inc., West Grove, PA, USA). The level of background fluorescence was determined by incubating sections in secondary antibody only. Apoptotic cells were identified with fluorescent terminal deoxynucleotidyl transferase–dUTP nick-end labeling (TUNEL) reagents (Roche Diagnostics, Mannheim, Germany). Coverslips were applied with Dapi Fluoro-Gel II Mounting Medium (Electron Microscopy Sciences, Hatfield, PA, USA).

Tissues were analyzed with the Nikon Eclipse E800 epifluorescence microscope (Nikon Instruments Inc., Melville, NY, USA) equipped with 10 x, 60 x, and 100 x lenses, the Infinity 3S camera (Teledyne DALSA, Waterloo, Ontario, Canada) and Image Pro Plus image analysis software program (Media Cybernetics, Rockville, MD, USA) and the Olympus Confocal Fluoview 1000 microscope equipped with a 60 x oil immersion lens and Fluoview software program (Olympus Corp., Tokyo, Japan). Adobe Photoshop version 23 (Adobe Inc., San Jose, CA, USA) was used to adjust photographs for brightness and contrast, and assembly and annotation of figures.

Quantitation of Fluorescently Labeled Cells and Statistical Analyses

Cells were scored for the presence of one or both fluorescent antibodies in ERMs, the retina, ciliary body, lens, cornea, and on the zonules of Zinn in each section. The number of α-SMA stained cells did not include smooth muscle surrounding blood vessels. The number of fluorescent cells in tissue

Table 1. Number of Cells Labeled With Antibodies to Markers of Myo/Nog Cells and Muscle in ERMs and the Retina

ERMs	**Grade**	**E/S**	**BAI1+/Noggin−**	**BAI1+/Noggin+**	**BAI1−/Noggin+**
	3/4	3/10	0	13 ± 4	0
	5/6	3/11	0	400 ± 258	0
	Grade	**E/S**	**BAI1+/α-SMA−**	**BAI1+/α-SMA+**	**BAI1−/α-SMA+**
	3/4	3/11	0.2 ± 0.6	10 ± 2	0
	5/6	3/13	80 ± 100	270 ± 124	0
	Grade	**E/S**	**BAI1+/Myosin−**	**BAI1+/Myosin+**	**BAI1−/Myosin+**
	3/4	4/17	5 ± 3	9 ± 8	0
	5/6	4/18	47 ± 18	98 ± 139	0.1 ± 0.2
Retina	**Grade**	**E/S**	**BAI1+/Noggin−**	**BAI1+/Noggin+**	**BAI1−/Noggin+**
	0	3/22	0	3 ± 1	0
	1-2	3/14	0	11 + 4	0
	3-4	3/8	0	12 ± 2	0
	5-6	3/11	0	106 ± 45	0
	Grade	**E/S**	**BAI1+/α-SMA−**	**BAI1+/α-SMA+**	**BAI1−/α-SMA+**
	0	3/11	6 ± 5	0	0
	1-2	3/14	5 ± 6	7 ± 5	0
	3-4	3/11	1 ± 2	13 ± 3	0
	5-6	3/13	5 ± 4	62 ± 43	0
	Grade	**E/S**	**BAI1+/Myosin−**	**BAI1+/Myosin+**	**BAI1−/Myosin+**
	0	3/12	7 ± 1	0	0
	1-2	3/15	10 ± 2	0	0
	3-4	4/30	3 ± 2	6 ± 7	0
	5-6	4/14	38 ± 14	23 ± 12	0

Sections were double labeled with the anti-BAI1 mAb and antibodies to noggin, α-SMA, and striated muscle myosin. Values are the mean ± standard deviation of double (+/+) and single labeled cells (+/− and −/+) in each section. The number of eyes (E) and sections (S) are indicated for each grade and pair of antibodies.

Investigative Ophthalmology & Visual Science

sections from PVR grades 1 and 2, 3 and 4, and 5 and 6 were combined to represent early retinal changes and moderate to severe PVR, respectively, as described above.[44] Data from eyes receiving intravitreal injections of 2000 to 8000 ARPE-19 cells were pooled for the same PVR grade.

The data represent the means and standard deviations of single and double labeled cells. The unpaired *t*-test was used to compare the means and standard deviations in different tissues as a function of PVR grade with a P value of ≤ 0.05 for statistical significance. Graphs were assembled with Prism GraphPad version 9.3.1. The percentage of Myo/Nog cells expressing muscle proteins was calculated by dividing the mean of the number of double labeled cells by the total number of BAI1+ cells and multiplying by 100.

Results

Myo/Nog Cells Increase in Response to Intravitreal Injection of Human RPE Cells and PVR Progression

Myo/Nog cells were localized in the eye by double labeling for BAI1 and noggin. All BAI1+ cells synthesized noggin and vice versa in the posterior and anterior segments in Grades 0-6 PVR (Tables 1, 2), thereby confirming their identity as Myo/Nog cells. Consistent with our previous study of murine eyes,[38] Myo/Nog cells were present in low numbers throughout the eye following intravitreal injections of PBS (PVR grade 0;)(see Tables 1, 2; Figs. 2A-C; Figs. 3A, 3B).

Table 2. Number of Cells Labeled With Antibodies to Markers of Myo/Nog Cells and Muscle in the Ciliary Body, Lens, and Cornea

Ciliary body	**Grade**	**E/S**	**BAI1+/Noggin−**	**BAI1+/Noggin+**	**BAI1−/Noggin+**
	0	3/19	0	0.2 ± 0.4	0
	1/2	3/14	0	1 ± 1	0
	3/4	3/7	0	9 ± 5	0
	5/6	3/11	0	18 ± 17	0
	Grade	**E/S**	**BAI1+/α-SMA−**	**BAI1+/α-SMA+**	**BAI1−/α-SMA+**
	0	3/11	1 ± 1	0	0
	1/2	3/14	0.4 ± 1	0.2 ± 0.4	0
	3/4	3/11	0.4 ± 1	11 ± 8	0
	5/6	3/13	1 ± 1	12 ± 10	0
	Grade	**E/S**	**BAI1+/Myosin−**	**BAI1+/Myosin+**	**BAI1−/Myosin+**
	0	3/12	1 ± 1	0	0
	1/2	3/17	5 ± 6	2 ± 3	0
	3/4	4/30	0.4 ± 1	0.1 ± 0.1	0
	5/6	4/18	5 ± 4	1 ± 3	0
Lens	**Grade**	**E/S**	**BAI1+/Noggin−**	**BAI1+/Noggin+**	**BAI1−/Noggin+**
	0	3/18	0	1 ± 1	0
	1-2	3/14	0	7 ± 6	0
	3-4	3/10	0	4 ± 3	0
	5-6	3/11	0	9 ± 8	0
	Grade	**E/S**	**BAI1+/α-SMA−**	**BAI1+/α-SMA+**	**BAI1−/α-SMA+**
	0	3/11	1 ± 1	0	0
	1-2	3/14	1 ± 1	4 ± 5	0
	3-4	3/11	0	2 ± 2	0
	5-6	3/13	0	10 ± 6	0
	Grade	**E/S**	**BAI1+/Myosin−**	**BAI1+/Myosin+**	**BAI1−/Myosin+**
	0	3/12	2 ± 1	0	0
	1-2	3/17	2 ± 1	0	0
	3-4	4/30	1 ± 1	0.2 ± 0.6*	0
	5-6	4/18	1 ± 1	0	0
Cornea	**Grade**	**E/S**	**BAI1+/Noggin−**	**BAI1+/Noggin+**	**BAI1−/Noggin+**
	0	3/21	0	1 ± 1	0
	1-2	3/14	0	11 + 11	0
	3-4	3/7	0	3 ± 3	0
	5-6	3/9	0	5 ± 5	0
	Grade	**E/S**	**BAI1+/α-SMA−**	**BAI1+/α-SMA+**	**BAI1−/α-SMA+**
	0	3/11	1 ± 1	0	0
	1-2	3/14	0.1 ± 0.3	8 ± 11	0
	3-4	3/11	0	1 ± 1	0
	5-6	3/13	0	2 ± 2	0
	Grade	**E/S**	**BAI1+/Myosin−**	**BAI1+/Myosin+**	**BAI1−/Myosin+**
	0	3/12	1 ± 1	0	0
	1-2	3/17	0.4 ± 1	0	0
	3-4	4/20	1 ± 2	0.3 ± 1	0
	5-6	4/18	2 ± 2	0	0

Sections were double labeled with the anti-BAI1 mAb and antibodies to noggin, α-SMA, and striated muscle myosin. Values are the mean ± standard deviation of double (+/+) and single labeled cells (+/− and −/+) in each section. The number of eyes (E) and sections (S) are indicated for each grade and pair of antibodies.

* External surface of the lens capsule.

Investigative Ophthalmology & Visual Science

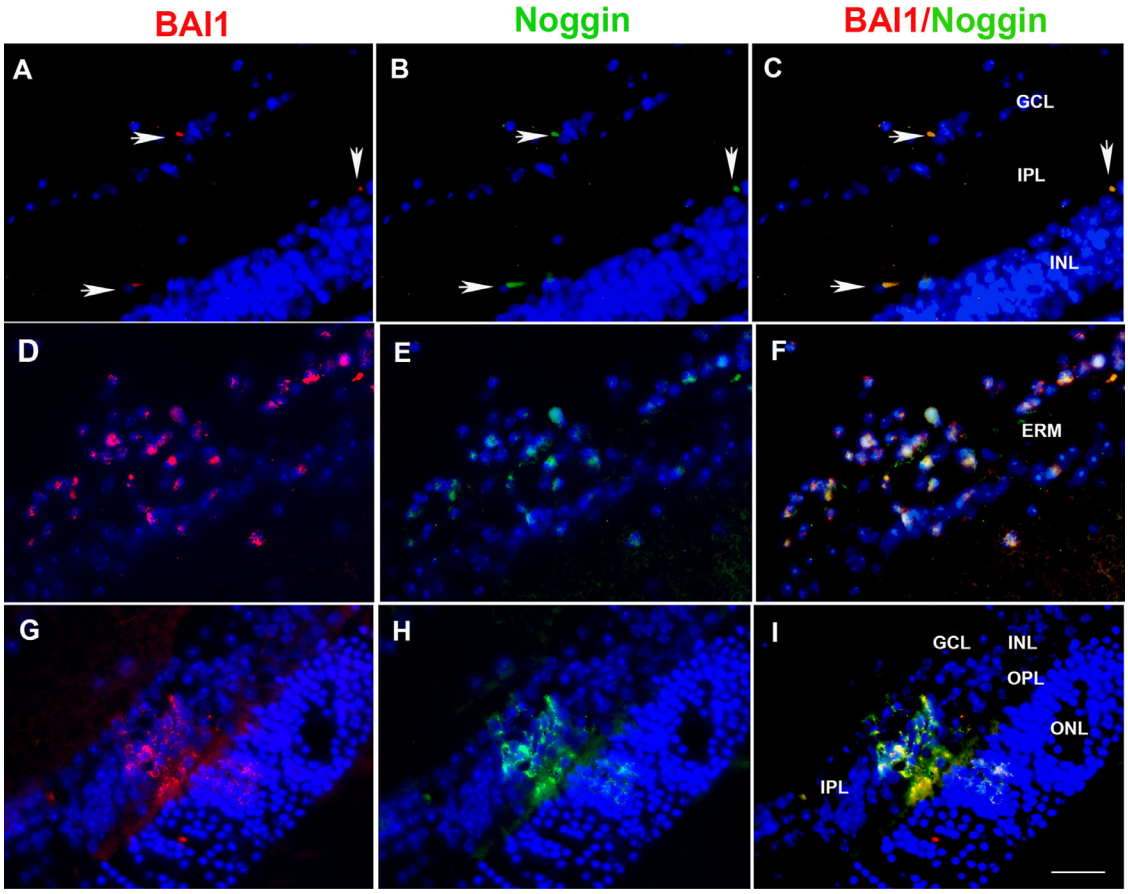

Figure 2. Localization of BAI1 and Noggin in ERMs and retina. Sections of mouse eyes with PVR grades 0 (**A-C**), 5 (**D-F**), and 3 (**G-I**) were double labeled with antibodies to BAI1 (*red*) and noggin (*green*). Nuclei were stained with DAPI (*blue*). The overlap of red and green appears yellow in merged images. BAI1 and noggin were co-localized in a small number of cells in the grade 0 retina **A** to -**C**. BAI1+/noggin+ cells were present throughout the ERM **D** to **F** and throughout the retina **G** to **I**. GCL = ganglion cell layer; IPL = inner plexiform layer; INL = inner nuclear layer; OPL = outer plexiform layer; ONL = outer nuclear layer. Bar = 9 µM.

The number of Myo/Nog cells increased significantly in the posterior segment with PVR progression (Figs. 2D-I; see Fig. 3A). Myo/Nog cells were present on the inner retinal surface (IRS) in grades 1/2 PVR and increased significantly in ERMs from approximately 54% to 72% of the total cells in ERMs between grades 3/4 and 5/6 ($P = 0.0025$; see Fig. 3A; Table 3). They were found in all layers of the retina (Figs. 2, 4, 5).

BAI1+ Myo/Nog cells also increased significantly in the anterior segment in response to PVR induction (see Fig. 3B). The peak of Myo/Nog cells in the lens and cornea was in eyes with PVR grades 1/2, and ciliary body and zonules of Zinn at grades 5/6 (see Fig. 3B). Although the number of Myo/Nog cells was increased in the anterior segment with intravitreal injection of ARPE-19 cells, the extent of the Myo/Nog cell response was minimal compared to posterior segment (see Figs. 3A, 3B; Tables 1, 2).

Muscle Proteins are Localized to Myo/Nog Cells

BAI1+ cells lacked detectable levels of α-SMA+ in grade 0 control eyes injected with PBS only (see Tables 1, 2). Injection of ARPE-19 cells stimulated the expression of α-SMA+ in Myo/Nog cells throughout the eye (see Tables 1, 2; Figs. 4A-H). In grades 3/4 and 5/6 ERMs, the percentages of BAI1+ cells containing α-SMA were approximately 98% and 77%, respectively (see Table 1). Within the retina, the percentage of BAI1+ cells with α-SMA increased from approximately 58% in grades 1/2 PVR to 93% in grades 3 to 6 (see Table 1). Most to all Myo/Nog cells in the ciliary body, lens, and cornea were labeled with the α-SMA by grades 3/4 (see Table 2). BAI1+/α-SMA+ cells were observed on the internal and external surfaces of the lens capsule (Figs. 5N-Q). Except for vascular smooth muscle cells, all α-SMA+ cells were co-labeled with the anti-BAI1 mAb in all ocular tissues and grades of PVR (see Tables 1, 2), including ERMs and the retina (see Figs. 4A-H).

No cells in the posterior and anterior segments were labeled with the mAb to striated muscle myosin II heavy chain in eyes injected with PBS (see Tables 1, 2). Striated muscle myosin was detected later in disease progression than α-SMA (see Tables 1, 2). Greater than 60% of BAI1+ cells were myosin+ in grades 3 to 6 ERMs (see Table 1; Figs. 4I-P). Only one myosin+ cell lacked BAI1 labeling in ERMs within 35 sections from 8 eyes (see Table 1).

BAI1+/myosin+ cells were present throughout the retina at higher PVR grades (see Figs. 4I-P). The approximate percentage of double labeled cells in grades 5/6 retinas was

Investigative Ophthalmology & Visual Science

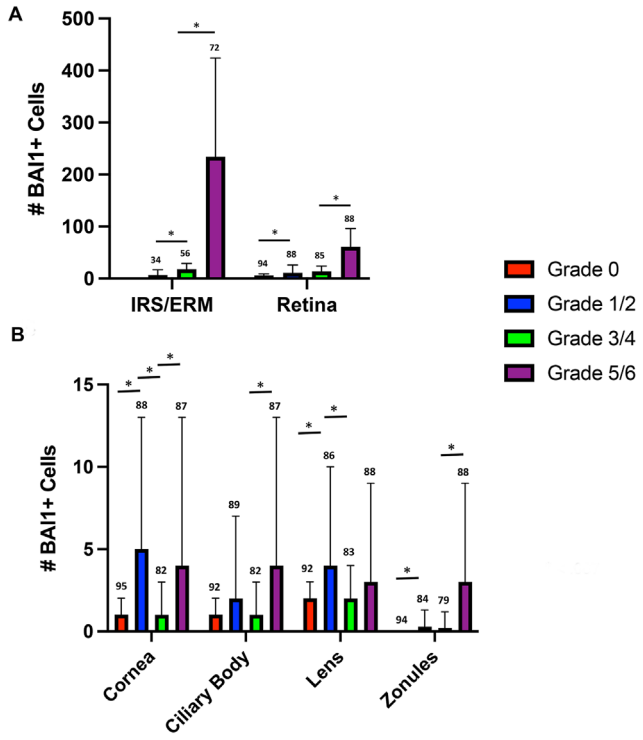

Figure 3. Number of BAI1+ cells per grade in a mouse model of PVR. Tissue sections of the eye were fluorescently labeled with the anti-BAI1 G8 mAb. The numbers of BAI1+ cells were counted in each section on the inner retinal surface (IRS; (grade 2), epiretinal membrane (ERM; grades 3–6), and retina (grades 0–6) (**A**), and the cornea, ciliary body, lens, and zonules of Zinn (grades 0–6) (**B**). The values are the mean ± standard deviation (SD) of the number of BAI1+ cells/section. The numbers of sections labeled with the BAI1 mAb are indicated above the SD bar. Grade 0 (injected with PBS): 9 eyes; grades 1/2: 7 eyes; grades 3/4 10 eyes; and grades 5/6: 13 eyes. * Indicates P values ≤ 0.004.

lower than grades 3/4, possibly reflecting a delay in myosin expression as the cells increase in number with disease progression (see Table 1). In most cases, retinal folds were overlain by ERMs enriched in α-SMA+ and striated myosin+ Myo/Nog cells (see Figs. 4A-D, I-L). BAI1+/myosin+ cells also were present in the ciliary body and on the external surface of the lens capsule in grades 3/4 (see Table 2). No double labeled cells were present in the cornea at any grade (see Table 2). All myosin+ cells expressed BAI1 in the retina and anterior segment (see Tables 1, 2). Only a single myosin-positive cell in lacked detectable BAI1 in 63 sections of grades 3 to 6 PVR. This cell was present in an ERM (see Table 1).

Table 3. Percentage of Myo/Nog Cells in Developing ERMs

Grade	# Eyes	# Sections	% Myo/Nog Cells
1/2	3	13	67 ± 18
3/4	12	32	54 ± 21
5/6	11	28	72 ± 21

The total number of cells identified with DAPI nuclear staining and total number of BAI1+ cells on the inner retinal surface (IRS) of grades 1/2 PVR and within grades 3 to 6 ERMs were counted in each section. % Myo/Nog cells on IRS and in ERMS = number of Myo/Nog cells ÷ total number of cells times 100. Results are the mean ± standard deviation.

Subpopulations of Myo/Nog Cells Express Leukocyte Markers

Tissue sections were labeled with antibodies to leukocyte markers to explore the possibility that injection of ARPE-19 cells elicited an inflammatory response which could contribute to the activation and migration of Myo/Nog cells and other cell types. CD68 is expressed in cells of the monocyte lineage, other myeloid cells, fibroblasts, and endothelial cells.[48,49] CD18 and CD45 are present in all leukocytes.[50,51] CD45 also was detected in peripheral blood insulin-producing cells.[52]

The labeling data for CD68, CD18, and CD45 is shown in Table 4. The numbers of leukocytes in the vitreous and retina were similar in eyes injected with PBS (grade 0) and ARPE-19 cells at grades 1/2 and increased slightly at higher grades. Low numbers of CD68+ and CD45+ cells were present in grades 1/2 and 3/4 ERMs. CD18+ cells were detected in ERMs by grades 5/6. CD45+ cells were more abundant than cells with CD68 or CD18 in grades 5 and 6 ERMs. Higher numbers of leukocytes were found in the cornea than the ciliary body. No CD68+, CD18+, or CD45+ cells were found in the lens at any grade.

Double labeling with the CD and BAI1 antibodies was performed to determine whether Myo/Nog cells expressed leukocyte markers (see Table 4). A maximum of 27% of Myo/Nog cells were labeled with CD antibodies in ERMs and fewer BAI1+ cells expressed CD18 than CD68 and CD45. All CD18+ and CD45+ cells in grades 5/6 ERMs contained BAI1. Less than 10% of Myo/Nog cells in the retina were labeled with the CD antibodies. In the vitreous, 14% to 33% of BAI1+ cells expressed CD68 and CD45 at grades 3/4 and no double labeled cells were found at grade 5/6. The cornea contained the highest percentages of BAI1+/CD+ cells. In this tissue, 67% of BAI1 cells were co-labeled with the CD68 mAb. CD+/BAI1- cells were found throughout the eye with the exception of CD18 in ERMs.

Distribution of Human and Pigmented Cells During Development of PVR

Sections were screened for ARPE-19 cells with an antibody to human nucleoli (hNuc). The specificity of the antibody was verified in sections of the human eye in which all nuclei were fluorescently labeled (not shown) and confirmed by the absence of labeling in mouse eyes injected with PBS (3 eyes and 11 sections). hNuc labeling was present in a total of 113 cells in the vitreous in 20 sections of grades 1/2 eyes, but not in the vitreous of grades 3 to 6 PVR (32 sections). None of the hNuc+ cells in the vitreous were labeled with the BAI1 mAb (see Fig. 5A). Some ARPE-19 cells were undergoing apoptosis as indicated by TUNEL staining (see Fig. 5B). Thirteen hNuc+ cells were found in a total of 18 sections of grades 3 to 6 ERMs. One hNuc+ nucleus appeared to be present in a cell separated from two unlabeled nuclei by BAI1 staining (see Figs. 5C-E). In the retina, no hNuc+ cells were found in 45 sections of grades 1 to 4 PVR and only 2 cells were labeled for hNuc in 9 sections of grades 5/6. These cells were negative for BAI1. The ciliary body, lens, and cornea lacked ARPE-19 cells at any grade.

Early in PVR development, a few pigmented cells were observed on the inner surface of the retina. An example of a cell with pigment, BAI1, a normal nucleus, and a dysmorphic nucleus is shown in Figure 5F and 5G. Grades 3 to 6 ERMs contained a subpopulation of pigmented cells among the

Investigative Ophthalmology & Visual Science

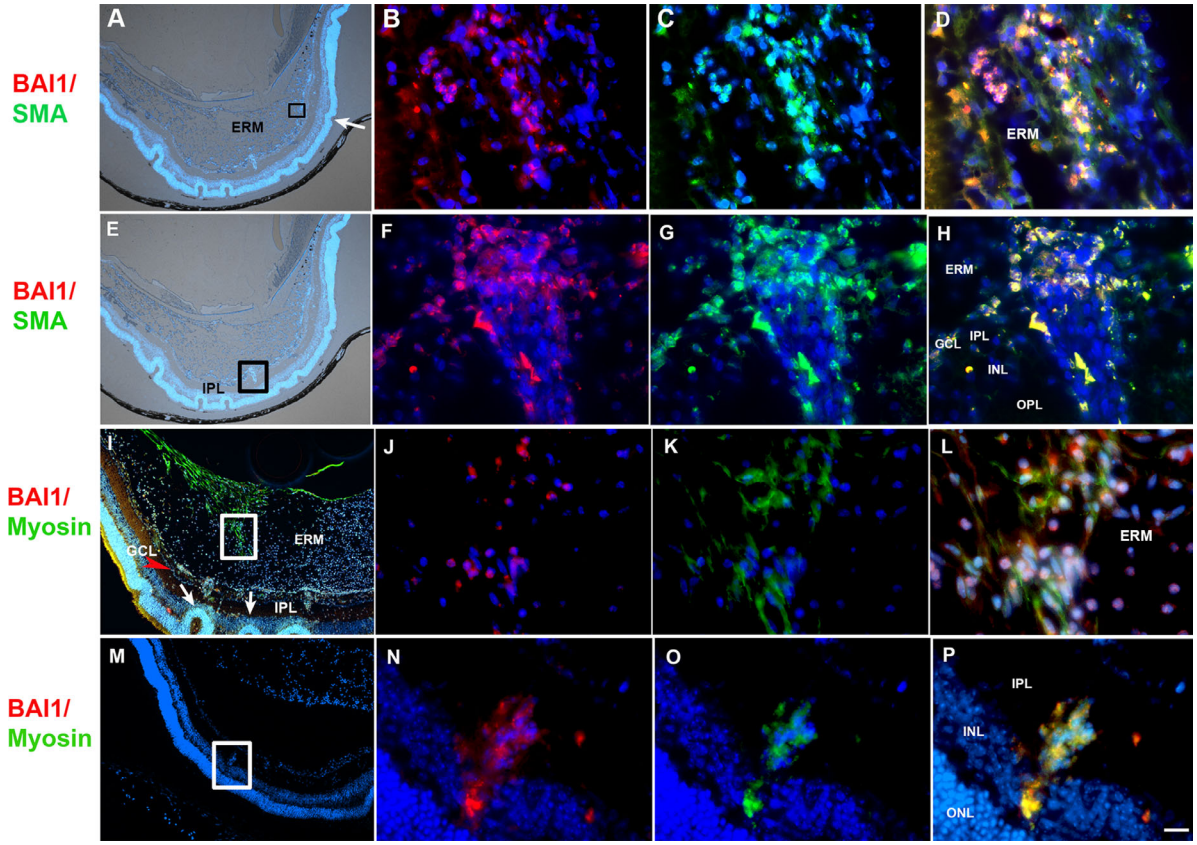

Figure 4. Localization of BAI1 and muscle proteins in ERMs and the retina. Sections of mouse eyes with PVR grades 5/6 were double labeled with antibodies to BAI1 (*red*) and α-SMA (*green*) (**A-H**) or striated muscle myosin (*green*) (**I-P**). Nuclei were stained with DAPI (*blue*). The overlap of *red* and *green* appears *yellow* in merged images (**D, H, L, P**). Regions within the boxes of the low magnification images in **A**, **E**, **I**, and **M** are shown at higher magnification in **B** to **D**, **F** to **H**, **J** to **L**, and **N** to **P**, respectively. BAI1 and α-SMA were co-localized in the ERM located in the vicinity of a retina fold (*arrow* in **A**). BAI1+/ α-SMA+ cells also were present throughout the layers of the retina (**E-H**). BAI1+/myosin+ cells were located within the ERM above the retinal folds (*white arrows* in **I**, **J-L**) and in the retina (**M-P**). ONL = outer nuclear layer; OPL = outer plexiform layer; INL = inner nuclear layer; IPL = inner plexiform layer; GCL = ganglion cell layer. Bar = 9 µM in **A** to **D**, **F** to **H**, **J** to **L**, and **N** and **O**, 57 µM in **I** and **M**, and 135 µM in **E**.

Myo/Nog cells (see Figs. 5H, 5Q). Pigmented cells invaded the retina from the RPE as PVR progressed (see Figs. 5I, R-U). In ERMs and the retina, pigmented cells resided either on the periphery (see Figs. 5H, M, Q, S) or among dense accumulations of BAI1+/myosin+ cells (see Fig. 5U). Noggin, α-SMA and striated myosin were not detected in cells with pigment (see Figs. 5J-M, N-Q, R-U, respectively). The zonules also contained pigmented cells (see Fig. 5M).

Discussion

The mouse model utilized in this study involves inducing PVR by detaching the posterior vitreous with gas and injecting ARPE-19 cells.[44] This model was adapted from a similar protocol used in rabbits to create a more cost-effective approach to drug testing and to study mechanisms in genetically modified animals.[44] Although the most common stimulus for PVR development (retinal tear or detachment) is not recapitulated in this model, key aspects of PVR pathogenesis, including dispersion of RPE cells into the vitreous cavity, ERM formation, and traction, are recreated with ARPE-19 cell injection. Generating reproducible retinal tears in a mouse or rabbit eye is technically challenging, and therefore, the majority of PVR models have incorporated the injection of cells (most commonly RPE cells) into the vitreous cavity to induce ERM formation with subsequent retinal detachment.[9,45] Our results with the ARPE-19 mouse model are similar to those we obtained with ERMs removed from patients that had a repair of a rhegmatogenous retinal detachment in which all cells with muscle proteins expressed Myo/Nog cell markers.[23]

Injection of ARPE-19 cells stimulated the expansion of the Myo/Nog cell population, identified by their co-expression of BAI1 and Noggin, in the posterior segment, and to a far lesser extent, the anterior segment. They were present on the retinal surface early in development of PVR (grades 1/2) and were the largest subpopulation of cells in ERMs. It is possible that the Myo/Nog cells on the retinal surface originated from those present in the ganglion cell or inner plexiform layer where they normally reside.[38,39] The ciliary body is another potential source of Myo/Nog cells, as evidenced by their expansion in this structure and migration on the zonules of Zinn in response to injection of ARPE-19 cells.

ARPE-19 cells, identified with an antibody to human nucleoli, were rare in ERMs, indicating that their induction of PVR was indirect. Their presence in the vitreous did not appear to elicit a large influx of CD+ leukocytes. In addition, the conjunctivas were white and quiet, and there were no signs of discomfort. These results suggest that

Investigative Ophthalmology & Visual Science

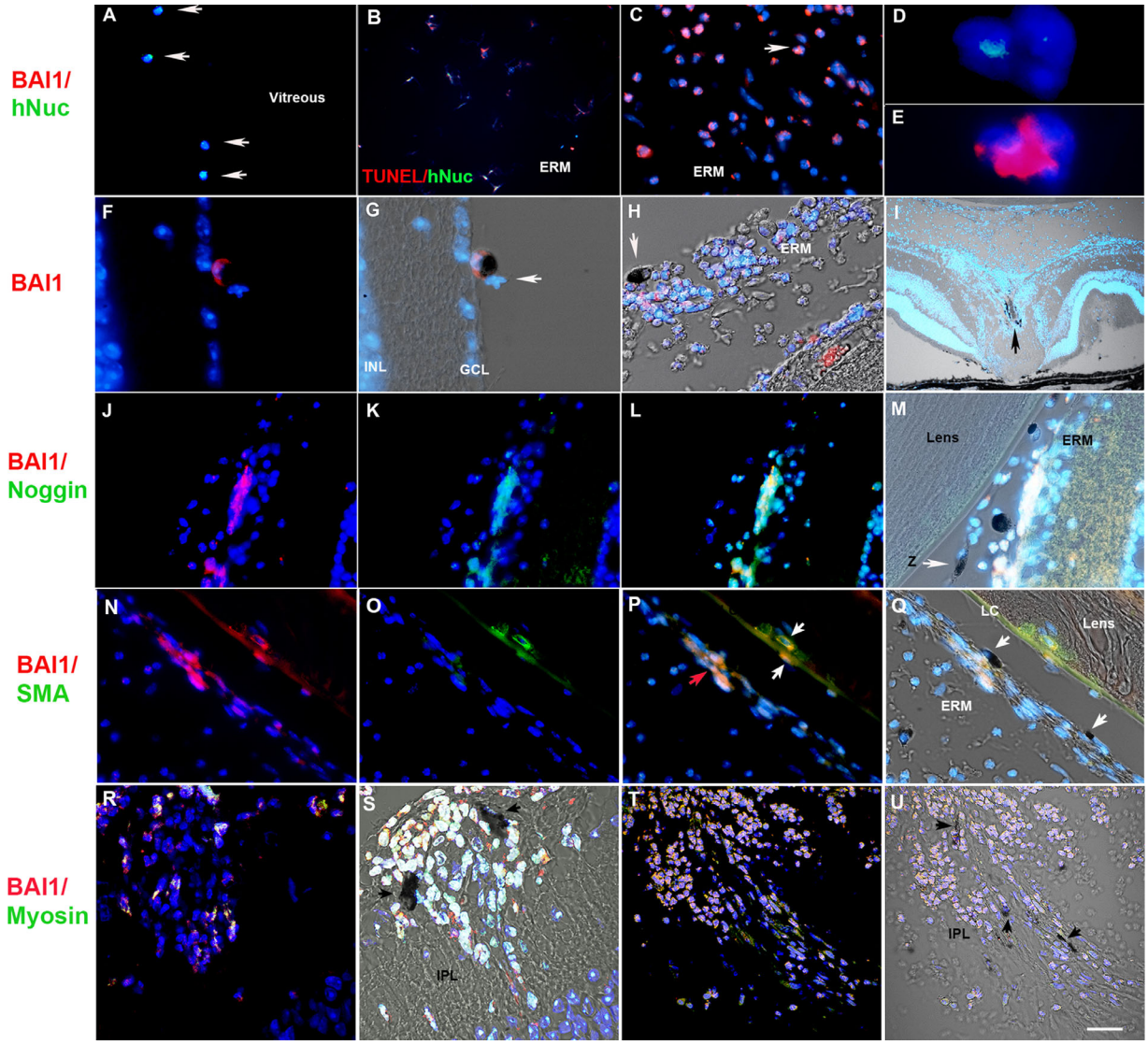

Figure 5. Localization of Myo/Nog, human, and pigmented cells in PVR. Sections of mouse eyes with PVR were double labeled with antibodies to BAI1 and hNuc (**A, C-E**), hNuc, and TUNEL reagents (**B**), and BAI1 and striated muscle myosin (**F-H**, **R-U**), noggin (**J-M**), or α-SMA (**N-Q**). The colors of the fluorescent secondary antibodies are indicated in the annotations. Nuclei were stained with DAPI (*blue*). The overlap of *red* and *green* appears *yellow* in merged images (**B**, **L**, **M**, **P**, **Q**, **R-U**). **G** to **-I**, **M**, **Q**, **S**, and **U** are merges of *red*, *green*, and/or *blue* and DIC. HNuc+ cells in the vitreous of grades 1/2 PVR were not labeled with the BAI1 mAb **A**. Some hNuc+ cells were apoptotic **B**. BAI1+ cells lacked detectable levels of hNuc in the ERM **C**. One hNuc+ nucleus appeared to be present in a cell with two other unlabeled nuclei (*arrow* in **C**, enlarged in **D** and **E**). BAI1 staining was between the three nuclei (**D**, **E**). BAI1 and pigment were present in a cell with a normal nucleus and a dysmorphic nucleus (**F**, **G**). A pigmented cell on the surface of a grade 5/6 ERM was surrounded by BAI1+/myosin- cells (*arrow* in **H**). A low magnification image shows pigmented cells that had invaded the retina (*arrow* in **I**). BAI1+/noggin+ cells in the grades 5/6 ERM did not contain pigment (**K-M**). Pigmented cells were visible on the zonule (*arrow* in **M**). BAI1 and α-SMA were co-localized in the ERM (*red arrow* in **P**) and on the internal and external surface of the lens capsule (**N-Q**, *white arrows* in **P**). Cells with pigment were present on the surface of the ERM (*arrows* in **Q**). Pigmented cells surrounded an aggregate of BAI1+/myosin+ cells in the retina (**R**, **S**) and were interspersed with differentiated Myo/Nog cells in grades 5/6 ERMs (**T**, **U**). INL = inner nuclear layer; IPL = inner plexiform layer; GCL = ganglion cell layer; Z = zonule. Bar = 9 µM in A-C, F-I and K-N, 10 µM in G and H; 57 µM in J, and 12 µM in O-R.

inflammation is not a significant trigger for the activation of Myo/Nog and other cell types, and the formation of ERMS in this model. An alternative stimulus for Myo/Nog cell activation are factors released from dying ARPE-19 cells that were revealed with TUNEL staining. Support for this hypothesis comes from our previous studies showing Myo/Nog cell accumulation in areas of cell death and their phagocytosis of cell corpses.[34,36,38,40,43]

Subpopulations of Myo/Nog cells expressed leukocyte markers, suggesting that they share mechanisms of response to disruptions in homeostasis with myeloid cells. Previously, we distinguished Myo/Nog cells from macrophages and microglia by the absence of staining with antibodies to Iba1 and F4/80 in the retina, brain and skin.[38,43,53,54] Not surprisingly, the CD68 marker for the monocyte lineage was found in some Myo/Nog cells. Both CD68 and BAI1 are receptors for phosphatidylserine (PS) present in the outer leaflet of the plasma membrane of apoptotic cells.[55–58] The binding of BAI1 to PS initiates phagocytosis,[57] a function of cells of the innate immune system and Myo/Nog cells.[43]

Investigative Ophthalmology & Visual Science

Table 4. Number of Cells Labeled With Antibodies to Leukocyte Markers in PVR

Tissue	BAI1+/CD68−	BAI1+/CD68+	BAI1−/CD68+	BAI1+/CD18−	BAI1+/CD18+	BAI1−/CD18+	BAI1+/CD45−	BAI1+/CD45+	BAI1−/CD45+
IRS/ERM									
G 1-2	16 ± 8 (7)	6 ± 5	0	1 ± 5 (26)	0	0	5 ± 4 (8)	0	0
G 3-4	19 ± 3 (9)	4 ± 4	0	19 ± 7 (5)	0	0	6 ± 3 (19)	0.3 ± 0.7	1 ± 2
G 5-6	121 ± 78 (9)	14 ± 8	4 ± 5	157 ± 39 (8)	20 ± 11	0	174 ± 44 (9)	59 ± 46	0
Retina									
G 0	6 ± 2 (11)	0.1 ± 0.3	0	7 ± 2 (15)	0	0	8 ± 2 (12)	0	0.2 ± 0.4
G 1-2	16 ± 3 (7)	0	0	10 ± 4 (26)	0.04 ± 0.2	0.1 ± 0.3	10 ± 12 (12)	0	0
G 3-4	24 ± 6 (12)	2 ± 3	0	16 ± 8 (15)	0	0	14 ± 6 (21)	0	1 ± 2
G 5-6	85 ± 14 (12)	4 ± 3	1 ± 1	37 ± 24 (12)	0	0	43 ± 9 (9)	3 ± 3	0.2 ± 0.6
Vitreous									
G 0	0 (7)	0	0	0 (11)	0	0	0 (8)	0	0
G 1-2	0 (7)	0	0	0.2 ± 0.4 (26)	0	0.1 ± 0.2	0 (4)	0	0
G 3-4	8 ± 9 (8)	4 ± 5	2 ± 3 (12)	1 ± 2 (9)	0	2 ± 2	3 ± 4 (17)	0.5 ± 1	3 ± 3
G 5-6	1 ± 2 (3)	0	5 ± 8	1 ± 1 (7)	0	0	0 (4)	0	8 ± 4
Cil Body									
G 0	1 ± 1 (11)	0	0	1 ± 1 (15)	0	1 ± 1	2 ± 1 (12)	0	0
G 1-2	3 ± 1 (7)	0.1 ± 0.3	0	2 ± 2 (26)	0	1 ± 1	3 ± 2 (13)	0	2 ± 5
G 3-4	1 ± 1 (12)	0	0	1 ± 1 (12)	0	2 ± 2	3 ± 2 (21)	0	0.1 ± 0.2
G 5-6	4 ± 2 (12)	1 ± 2	1 ± 1	6 ± 4 (16)	0.3 ± 0.5	0	6 ± 3 (10)	1 ± 2	0
Lens									
G 0	1 ± 1 (11)	0	0	3 ± 1 (26)	0	0	1 ± 1 (12)	0	0
G 1-2	1 ± 1 (7)	0	0	3 ± 1 (14)	0	0	7 ± 9 (12)	0	0
G 3-4	1 ± 1 (9)	0	0	1 ± 2 (9)	0	0	6 ± 7 (21)	0	0
G 5-6	1 ± 1 (12)	0	0	1 ± 1 (12)	0	0	1 ± 1 (13)	0	0
Cornea									
G 0	1 ± 1 (11)	0.3 ± 0.4	1 ± 2	2 ± 2 (26)	0.1 + 0.4	1 ± 1	1 ± 1 (12)	0	4 ± 4
G 1-2	1 ± 1 (7)	2 ± 2	6 ± 3	3 ± 1 (14)	0.2 ± 0.6	2 ± 2	5 ± 7 (12)	6 ± 1	3 ± 5
G 3-4	1 + 1 (12)	0.1 ± 0.3	2 ± 2	0.3 ± 0.6 (11)	0	6 ± 8	5 ± 5 (21)	1 ± 1	6 ± 4
G 5-6	1 ± 1 (12)	2 ± 3	1 ± 1	5 ± 7 (12)	9 ± 13	0	0 (13)	0	2 ± 2

Sections were double labeled with the anti-BAI1 mAb and antibodies to CD 68, CD 18, and CD45. Values are the mean ± standard deviation of double (+/+) and single labeled cells (+/− and −/+) in each section. The numbers of sections scored are indicated in parentheses. Sections from 3 eyes were scored for all grades 0 and grades 3/4 and grades 5/6 CD45. Sections from 4 eyes were scored for all grades 1/2 and grades 3/4 CD18 and CD68. IRS = inner retinal surface.

Engulfment of pigmented and human cells was suggested by the appearance of cells with BAI1, a dysmorphic nucleus and pigment, or a human nucleolus.

Pigmented cells were present along with Myo/Nog cells in all grades of PVR. It is unclear how pigmented cells from the mouse RPE would reach the inner surface of the retina during early stages of PVR in the absence of a tear. However, RPE cells have been identified in idiopathic ERMs in patients without tears and OCT data has demonstrated evidence of transretinal migration of RPE cells.[59,60] Other possible sources of pigmented cells seen on the retinal surface and ERMs are the anterior margin of the RPE and ciliary body.[22] At higher PVR grades, pigmented cells presumably migrating from the RPE extended from the outer retina into the ERM. Lineage tracing with stably expressed reporters will be required to define the origins of pigmented cells with PVR progression.

Induction of PVR stimulated the expression of α-SMA only in BAI1+ Myo/Nog cells. Progression of myogenic differentiation was revealed by their synthesis of striated muscle specific myosin II. BAI1, noggin, α-SMA, and striated myosin+ myofibroblasts were often associated with retinal folds. These findings demonstrate that Myo/Nog cells are the source of myofibroblasts in ERMs. Given the abundance of differentiated Myo/Nog cells in the retina in advanced disease, they are likely contributors to intraretinal fibrosis that occurs in some cases of PVR.[1,5,8]

Contractile myofibroblasts in PVR membranes have been postulated to arise from a variety of sources, including RPE and glial cells that transdifferentiate into muscle cells.[1,4,5,10,13,15–22] RPE and Muller cells synthesize α-SMA in culture and can produce a tractional force on a collagen gel.[61–67] The most compelling evidence for RPE cells as the source of myofibroblasts in PVR was co-localization of α-SMA and cytokeratin-18, a marker of epithelial cells, in human ERMs.[17] This study also demonstrated co-expression of α-SMA and the Muller and astrocyte cell marker glial fibrillary acidic protein (GFAP). To our knowledge, it has not been reported that expression of α-SMA is sufficient for contraction or whether additional muscle proteins are synthesized in either RPE or glia cells in vitro or in vivo. Knockdown of α-SMA did not prevent contractions in cultures of lens cells.[68]

We cannot rule out the possibility that mouse RPE cells lost pigment following an epithelial to mesenchymal transition and transdifferentiated into cells that express BAI1, noggin, and muscle proteins. It also is possible that glial cells transdifferentiated into Myo/Nog cells. However, we favor the hypothesis that myofibroblasts arose directly from Myo/Nog cells for the following reasons. First, Myo/Nog cells normally reside within the retina and other ocular tissues, are activated by multiple forms of stress and injury, are inherently myogenic, and stably committed to the skeletal muscle lineage regardless of their environment.[31–33,38,39,69] They are the primary, if not exclusive source of noggin in the embryo and adult, including the eyes.[23,25,31,33,35,37–39,69] Noggin expression defines the Myo/Nog cells lineage and is not a characteristic of all differentiating myoblasts.[25] Furthermore, Myo/Nog cells do not express cytokeratins in skin tumors and surrounding tissues.[36] Pigmented cells within the ciliary body epithelium, RPE, human ERMs, and in this mouse model of PVR do not express detectable levels of BAI1, noggin, MyoD, α-SMA, or striated muscle myosin,[23,33,38,39,69] although, if they retained pigment, they may not have fully transdifferentiated. Neither BAI1 nor noggin were detected in the RPE or Muller and other glia cells in retinopathy induced by hypoxia and light damage, and GFAP was not present in Myo/Nog cells.[38,39] Although fibroblasts also were postulated to be a source of myofibroblasts in ERMs,[70] Myo/Nog cells have a fibroblast-like morphology. Whereas multiple cell types clearly contribute to ERM formation, we conclude that Myo/Nog cells are the source of myofibroblasts within the membranes and retina, and generators of a tractional force that causes folds and detachment.

Depletion of Myo/Nog cells with intravitreal injections of a cytotoxic drug specifically targeted to BAI1 will reveal whether this is a viable approach for preventing ERM formation and retinal detachment, as it was for preventing the accumulation of myofibroblasts and mitigating PCO in response to cataract surgery in rabbits.[33] Cataract surgery with phacoemulsification and an abnormal vitreoretinal interface is a risk factor for retinal detachment and the onset or progression of ERM formation.[71,72] It is possible that Myo/Nog cell activation in the lens and ciliary body could result in their migration and contribution to ERM formation.

A potential complication of targeting Myo/Nog cells in the retina is related to their neuroprotective function. Depletion of Myo/Nog cells increased photoreceptor cell death in a mouse model of oxygen induced retinopathy, and addition of Myo/Nog cells to the rat vitreous following light damage promoted photoreceptor survival and function.[38,39] However, killing Myo/Nog cells in the normal retina did not affect neuronal viability, suggesting that their neuroprotective function becomes important when the retina is compromised.[38] Therefore, the absence of Myo/Nog cells may not be detrimental to neurons if ERM formation and retinal detachment are prevented. Myo/Nog cells continue to express BAI1 after differentiating into myofibroblasts (current study and refs. [23,33]). Depleting Myo/Nog cells could be a strategy for treating existing membranes before the development of retinal tears and detachment, in addition to preventing ERM formation in patients who are at high risk of developing PVR.

Acknowledgments

The authors thank Joseph F. Richards for his assistance with labeling tissue sections.

Supported by an anonymous Myo/Nog cell program project award to MG-W and ABN, a Research to Prevent Blindness Unrestricted Grant (A.E.K.), NIHP30EY001319 (David Williams, Center for Visual Sciences [A.E.K.], Alcon Research Institute Young Investigator Grant (A.E.K.) and Macula Society Young Investigator Grant (A.E.K.).

Discloser: **M. Crispin**, None; **J. Gerhart**, None; **A. Heffer**, None; **M. Martin**, None; **F. Abdalla**, None; **A. Bravo-Nuevo**, None; **N.J. Philp**, None; **A.E. Kuryan**, Consultant/Speaker: Alimera Sciences, Allergan, Bausch + Lomb, Optos, Novartis, Genentech/Roche, Regeneron, Recens Medical, Spark Therapeutics; Grant funding: Adverum, Alcon, Annexon, Genentech/Roche, Second Sight; **M. George-Weinstein**, None

References

1. Idrees S, Sridhar J, Kuriyan AE. Proliferative Vitreoretinopathy: A Review. *Int Ophthalmol Clin*. 2019;59:221–240.
2. Pastor JC. Proliferative vitreoretinopathy: an overview. *Surv Ophthalmol*. 1998;43:3–18.

3. Shahlaee A, Woeller CF, Philp NJ, Kuriyan AE. Translational and clinical advancements in management of proliferative vitreoretinopathy. *Curr Opin Ophthalmol*. 2022;33:219–227.
4. Glaser BM, Cardin A, Biscoe B. Proliferative vitreoretinopathy. The mechanism of development of vitreoretinal traction. *Ophthalmology*. 1987;94:327–332.
5. Pastor JC, de la Rua ER, Martin F. Proliferative vitreoretinopathy: risk factors and pathobiology. *Prog Retin Eye Res*. 2002;21:127–144.
6. Morescalchi F, Duse S, Gambicorti E, Romano MR, Costagliola C, Semeraro F. Proliferative vitreoretinopathy after eye injuries: an overexpression of growth factors and cytokines leading to a retinal keloid. *Mediators Inflamm*. 2013;2013:269787.
7. Nagasaki H, Shinagawa K, Mochizuki M. Risk factors for proliferative vitreoretinopathy. *Prog Retin Eye Res*. 1998;17:77–98.
8. Khan MA, Brady CJ, Kaiser RS. Clinical management of proliferative vitreoretinopathy: an update. *Retina* .2015;35:165–175.
9. Hou H, Nudleman E, Weinreb RN. Animal Models of Proliferative Vitreoretinopathy and Their Use in Pharmaceutical Investigations. *Ophthalmic Res*. 2018;60:195–204.
10. Amarnani D, Machuca-Parra AI, Wong LL, et al. Effect of Methotrexate on an In Vitro Patient-Derived Model of Proliferative Vitreoretinopathy. *Invest Ophthalmol Vis Sci*. 2017;58:3940–3949.
11. Garweg JG, Tappeiner C, Halberstadt M. Pathophysiology of proliferative vitreoretinopathy in retinal detachment. *Surv Ophthalmol*. 2013;58:321–329.
12. Tosi GM, Marigliani D, Romeo N, Toti P. Disease pathways in proliferative vitreoretinopathy: an ongoing challenge. *J Cell Physiol*. 2014;229:1577–1583.
13. Jerdan JA, Pepose JS, Michels RG, et al. Proliferative vitreoretinopathy membranes. An immunohistochemical study. *Ophthalmology*. 1989;96:801–810.
14. Kampik A, Kenyon KR, Michels RG, Green WR, de la Cruz ZC. Epiretinal and vitreous membranes. Comparative study of 56 cases. *Arch Ophthalmol*. 1981;99:1445–1454.
15. Morino I, Hiscott P, McKechnie N, Grierson I. Variation in epiretinal membrane components with clinical duration of the proliferative tissue. *Br J Ophthalmol*. 1990;74:393–399.
16. Sramek SJ, Wallow IH, Stevens TS, Nork TM. Immunostaining of preretinal membranes for actin, fibronectin, and glial fibrillary acidic protein. *Ophthalmology*. 1989;96:835–841.
17. Feist RM, King JL, Morris R, Witherspoon CD, Guidry C. Myofibroblast and extracellular matrix origins in proliferative vitreoretinopathy. *Graefes Arch Clin Exp Ophthalmol*. 2014;252:347–357.
18. Oberstein SY, Byun J, Herrera D, Chapin EA, Fisher SK, Lewis GP. Cell proliferation in human epiretinal membranes: characterization of cell types and correlation with disease condition and duration. *Mol Vis*. 2011;17:1794–1805.
19. Kroll P, Rodrigues EB, Hoerle S. Pathogenesis and classification of proliferative diabetic vitreoretinopathy. *Ophthalmologica*. 2007;221:78–94.
20. Asaria RH, Charteris DG. Proliferative vitreoretinopathy: developments in pathogenesis and treatment. *Compr Ophthalmol Update*. 2006;7:179–185.
21. Bochaton-Piallat ML, Kapetanios AD, Donati G, Redard M, Gabbiani G, Pournaras CJ. TGF-beta1, TGF-beta receptor II and ED-A fibronectin expression in myofibroblast of vitreoretinopathy. *Invest Ophthalmol Vis Sci*. 2000;41:2336–2342.
22. Baudouin C, Fredj-Reygrobellet D, Gordon WC, et al. Immunohistologic study of epiretinal membranes in proliferative vitreoretinopathy. *Am J Ophthalmol*. 1990;110:593–598.
23. Gerhart J, Morrison N, Gugerty L, Telander D, Bravo-Nuevo A, George-Weinstein M. Myo/Nog cells expressing muscle proteins are present in preretinal membranes from patients with proliferative vitreoretinopathy. *Exp Eye Res*. 2020;197:108080.
24. Sirpa L, Ani K, Markku V, Erika G. Vitreal protein myogenic factor 6 is increased in eyes with rhegmatogenous retinal detachment. *Acta Ophthalmol*. 2022;100(8):e1767–e1768.
25. Gerhart J, Elder J, Neely C, et al. MyoD-positive epiblast cells regulate skeletal muscle differentiation in the embryo. *J Cell Biol*. 2006;175:283–292.
26. Gerhart J, Baytion M, DeLuca S, et al. DNA dendrimers localize MyoD mRNA in presomitic tissues of the chick embryo. *J Cell Biol*. 2000;149:825–834.
27. Gerhart J, Neely C, Stewart B, et al. Epiblast cells that express MyoD recruit pluripotent cells to the skeletal muscle lineage. *J Cell Biol*. 2004;164:739–746.
28. Strony R, Gerhart J, Tornambe D, et al. NeuroM and MyoD are expressed in separate subpopulations of cells in the pregastrulating epiblast. *Gene Expr Patterns*. 2005;5:387–395.
29. Gerhart J, Bowers J, Gugerty L, et al. Brain-specific angiogenesis inhibitor 1 is expressed in the Myo/Nog cell lineage. *PLoS One*. 2020;15:e0234792.
30. Gerhart J, Bast B, Neely C, et al. MyoD-positive myoblasts are present in mature fetal organs lacking skeletal muscle. *J Cell Biol*. 2001;155:381–392.
31. Gerhart J, Greenbaum M, Scheinfeld V, et al. Myo/Nog cells: targets for preventing the accumulation of skeletal muscle-like cells in the human lens. *PLoS One*. 2014;9:e95262.
32. Gerhart J, Neely C, Elder J, et al. Cells that express MyoD mRNA in the epiblast are stably committed to the skeletal muscle lineage. *J Cell Biol*. 2007;178:649–660.
33. Gerhart J, Werner L, Mamalis N, et al. Depletion of Myo/Nog Cells in the Lens Mitigates Posterior Capsule Opacification in Rabbits. *Invest Ophthalmol Vis Sci*. 2019;60:1813–1823.
34. Gerhart J, Scheinfeld VL, Milito T, et al. Myo/Nog cell regulation of bone morphogenetic protein signaling in the blastocyst is essential for normal morphogenesis and striated muscle lineage specification. *Dev Biol*. 2011;359:12–25.
35. Gerhart J, Pfautz J, Neely C, et al. Noggin producing, MyoD-positive cells are crucial for eye development. *Dev Biol*. 2009;336:30–41.
36. Gerhart J, Hayes C, Scheinfeld V, Chernick M, Gilmour S, George-Weinstein M. Myo/Nog cells in normal, wounded and tumor-bearing skin. *Exp Dermatol*. 2012;21:466–468.
37. Gerhart J, Behling K, Paessler M, et al. Rhabdomyosarcoma and Wilms tumors contain a subpopulation of noggin producing, myogenic cells immunoreactive for lens beaded filament proteins. *PLoS One*. 2019;14:e0214758.
38. Bravo-Nuevo A, Brandli AA, Gerhart J, et al. Neuroprotective effect of Myo/Nog cells in the stressed retina. *Exp Eye Res*. 2016;146:22–25.
39. Brandli A, Gerhart J, Sutera CK, et al. Role of Myo/Nog Cells in Neuroprotection: Evidence from the Light Damaged Retina. *PLoS One*. 2017;12:e0169744.
40. Joseph-Pauline S, Morrison N, Braccia M, et al. Acute Response and Neuroprotective Role of Myo/Nog Cells Assessed in a Rat Model of Focal Brain Injury. *Front Neurosci*. 2021;15:780707.
41. Wormstone IM, Wang L, Liu CS. Posterior capsule opacification. *Exp Eye Res*. 2009;88:257–269.
42. Gerhart J, Greenbaum M, Casta L, et al. Antibody-Conjugated, DNA-Based Nanocarriers Intercalated with Doxorubicin Eliminate Myofibroblasts in Explants of Human Lens Tissue. *J Pharmacol Exp Ther*. 2017;361:60–67.

Investigative Ophthalmology & Visual Science

43. Gerhart J, Gugerty L, Lecker P, et al. Myo/Nog cells are nonprofessional phagocytes. *PLoS One*. 2020;15:e0235898.
44. Heffer A, Wang V, Sridhar J, et al. A Mouse Model of Proliferative Vitreoretinopathy Induced by Intravitreal Injection of Gas and RPE Cells. *Transl Vis Sci Technol*. 2020;9:9.
45. Agrawal RN, He S, Spee C, Cui JZ, Ryan SJ, Hinton DR. In vivo models of proliferative vitreoretinopathy. *Nature Protocols*. 2007;2:67–77.
46. Dunn KC, Aotaki-Keen AE, Putkey FR, Hjelmeland LM. ARPE-19, a human retinal pigment epithelial cell line with differentiated properties. *Exp Eye Res*. 1996;62:155–169.
47. Fastenberg DM, Diddie KR, Sorgente N, Ryan SJ. A comparison of different cellular inocula in an experimental model of massive periretinal proliferation. *Am J Ophthalmol*. 1982;93:559–564.
48. Gottfried E, Kunz-Schughart LA, Weber A, et al. Expression of CD68 in non-myeloid cell types. *Scand J Immunol*. 2008;67:453–463.
49. Ramprasad MP, Terpstra V, Kondratenko N, Quehenberger O, Steinberg D. Cell surface expression of mouse macrosialin and human CD68 and their role as macrophage receptors for oxidized low density lipoprotein. *Proc Natl Acad Sci USA*. 1996;93:14833–14838.
50. Grindem CB. Blood cell markers. *Vet Clin North Am Small Anim Pract*. 1996;26:1043–1064.
51. Danilenko DM, Moore PF, Rossitto PV. Canine leukocyte cell adhesion molecules (LeuCAMs): characterization of the CD11/CD18 family. *Tissue Antigens*. 1992;40:13–21.
52. Rheinlander A, Schraven B, Bommhardt U. CD45 in human physiology and clinical medicine. *Immunol Lett*. 2018;196:22–32.
53. Gerhart J, Hayes C., Scheinfeld V., Chernick M., Gilmour S., George-Weinstein M.. Myo/Nog cells in normal, wounded and tumor bearing skin. *Exp Dermatol*. 2012;21:466–468.
54. Gerhart J, Bowers J., Gugerty L., et al. Brain-specific angiogenesis inhibitor 1 is expressed in the Myo/Nog cell lineage. *PLos One*. 2020;15(7)e0234792.
55. Sokolowski JD, Nobles SL, Heffron DS, Park D, Ravichandran KS, Mandell JW. Brain-specific angiogenesis inhibitor-1 expression in astrocytes and neurons: implications for its dual function as an apoptotic engulfment receptor. *Brain Behav Immun*. 2011;25:915–921.
56. Park D, Tosello-Trampont AC, Elliott MR, et al. BAI1 is an engulfment receptor for apoptotic cells upstream of the ELMO/Dock180/Rac module. *Nature*. 2007;450:430–434.
57. Hochreiter-Hufford AE, Lee CS, Kinchen JM, et al. Phosphatidylserine receptor BAI1 and apoptotic cells as new promoters of myoblast fusion. *Nature*. 2013;497:263–267.
58. Sambrano GR, Steinberg D. Recognition of oxidatively damaged and apoptotic cells by an oxidized low density lipoprotein receptor on mouse peritoneal macrophages: role of membrane phosphatidylserine. *Proc Natl Acad Sci USA*. 1995;92:1396–1400.
59. Smiddy WE, Maguire AM, Green WR, et al. Idiopathic epiretinal membranes. Ultrastructural characteristics and clinicopathologic correlation. *Ophthalmology*. 1989;96:811–820; discussion 821.
60. Zacks DN, Johnson MW. Transretinal pigment migration: an optical coherence tomographic study. *Arch Ophthalmol*. 2004;122:406–408.
61. Guidry C, Bradley KM, King JL. Tractional force generation by human muller cells: growth factor responsiveness and integrin receptor involvement. *Invest Ophthalmol Vis Sci*. 2003;44:1355–1363.
62. Grisanti S, Guidry C. Transdifferentiation of retinal pigment epithelial cells from epithelial to mesenchymal phenotype. *Invest Ophthalmol Vis Sci*. 1995;36:391–405.
63. Guidry C. Isolation and characterization of porcine Muller cells. Myofibroblastic dedifferentiation in culture. *Invest Ophthalmol Vis Sci*. 1996;37:740–752.
64. Kurosaka D, Muraki Y, Inoue M, Katsura H. TGF-beta 2 increases alpha-smooth muscle actin expression in bovine retinal pigment epithelial cells. *Curr Eye Res*. 1996;15:1144–1147.
65. Ando A, Ueda M, Uyama M, Masu Y, Ito S. Enhancement of dedifferentiation and myoid differentiation of retinal pigment epithelial cells by platelet derived growth factor. *Br J Ophthalmol*. 2000;84:1306–1311.
66. Si Y, Wang J, Guan J, Han Q, Hui Y. Platelet-derived growth factor induced alpha-smooth muscle actin expression by human retinal pigment epithelium cell. *J Ocul Pharmacol Ther*. 2013;29:310–318.
67. Stocks SZ, Taylor SM, Shiels IA. Transforming growth factor-beta1 induces alpha-smooth muscle actin expression and fibronectin synthesis in cultured human retinal pigment epithelial cells. *Clin Exp Ophthalmol*. 2001;29:33–37.
68. Dawes LJ, Eldred JA, Anderson IK, et al. TGF beta-induced contraction is not promoted by fibronectin-fibronectin receptor interaction, or alpha SMA expression. *Invest Ophthalmol Vis Sci*. 2008;49:650–661.
69. Gerhart J, Withers C, Gerhart C, et al. Myo/Nog cells are present in the ciliary processes, on the zonule of Zinn and posterior capsule of the lens following cataract surgery. *Exp Eye Res*. 2018;171:101–105.
70. Vinores SA, Campochiaro PA, McGehee R, Orman W, Hackett SF, Hjelmeland LM. Ultrastructural and immunocytochemical changes in retinal pigment epithelium, retinal glia, and fibroblasts in vitreous culture. *Invest Ophthalmol Vis Sci*. 1990;31:2529–2545.
71. Qureshi MH, Steel DHW. Retinal detachment following cataract phacoemulsification-a review of the literature. *Eye (Lond)*. 2020;34:616–631.
72. Kwon S, Kim B, Jeon S. Risk factors for onset or progression of epiretinal membrane after cataract surgery. *Sci Rep*. 2021;11:14808.

Investigative Ophthalmology & Visual Science